Performance Assessment of an Electrical Impedance Tomography Detector for Mine-Like Objects

Philip M. Church, Neptec Design Group*, Philip M. Wort, Zenastra**, Stephane Gagnon, PMC Sierra***, John McFee, Defence Research Establishment Suffield****

ABSTRACT

This paper reports the results of the performance assessment of an Electrical Impedance Tomography detector (EIT) for mine-like objects in soils. EIT uses an array of electrodes to inject low frequency currents in the soil and measure the resulting electrical potentials. The measurements are then used to reconstruct the electrical conductivity perturbations underneath the array. In the course of this work, an EIT instrument was built and field evaluated. The array is made of 64 stainless steel stimulating and recording electrodes arranged in an 8x8 grid. Specialized electronics has been built to control the electrode current stimulations and potential measurements. The detection algorithm is tuned to objects of a given size and shape to reduce the false alarm rate. The main mechanical, electronic and algorithm components of the detector will be presented.

The EIT detector was originally designed in view of evaluating its potential as a confirmatory detector of AT mines. To that end, mine-like objects representative of some AT mines were used. Results of preliminary field evaluations are presented. The detection capabilities and limitations of mine-like objects are discussed.

Keywords: EIT, landmine, detection, electrode.

1. INTRODUCTION

Electrical Impedance Tomography (EIT) is a technology developed to image the electrical conductivity distribution of a conductive medium. The technology is of interest because of its low cost and also because the measurement of the electrical conductivity brings direct information about the composition of the conductive medium.

The EIT technology is relatively recent and has been researched mostly for medical diagnostic applications. Since the ground is conductive to a certain extent, the technology can also be used to detect buried objects. The application of landmine detection is of particular interest because the object is usually buried at shallow depths and causes a discontinuity in the soil conductivity.

The research done in the application of EIT to detect landmines has been very limited. Wexler was one of the first investigators to apply EIT to the detection of Unexploded Ordnance (UXO) in the ground, with limited success [1], [2]. The detection of UXO requires probing depths that are large relative to the size of the surface electrode array and EIT may not be the best technology for this particular application. The EIT technology is sensitive to noise, which prevents its use at depths that are large with respect to the electrode array size. It holds promises, however, when the problem is constrained to the detection of objects buried at shallow depths, such as landmines. The original objective of this research was to assess, as a first step, the feasibility of using the EIT technology as the basis of a confirmatory Anti-Tank (AT) mine detector. Under the sponsorship of the Defence Research Establishment Suffield (DRES), an initial research phase (Phase 1) had determined through lab experiments that the two major technical risks perceived for that technology, namely the reliability of the electrode-soil contact and the reconstruction algorithm, were surmountable. A description of the work performed during Phase 1 can be found in [3].

---

* pchurch@neptec.com; phone (613) 599-7603 (x513); fax (613) 599-7604; Neptec Design Group, 302 Legget Dr., Kanata, Ont., Canada, K2K 1Y5; ** philip.wort@zenastra.com; phone (613) 736-8777 (x289); Zenastra Photonics, 2305 St-Laurent, Ottawa, Ont., Canada, K1G 4J8; ***sgagnon@pmc-sierra.com; phone (613) 599-6088 PMC-Sierra, 411 Legget Dr., Kanata, Ont., Canada, K2K 3C9; ****

The work reported in this paper represents the next phase (Phase 2) of the research work. Its main objective was to build an EIT landmine detector aimed at AT landmines and perform some initial field evaluations. The design of the detector and its detection performance in a few environments is described in the following sections.

2. EIT INSTRUMENT

Electrical Impedance Tomography uses low-level electrical currents to probe a conductive medium and produce an image of its electrical conductivity distribution. While a pair of electrodes is stimulated, the electrical voltage is measured on the remaining pairs of electrodes. After all the independent combinations of interest have been stimulated, an algorithm using the measured data reconstructs an image of the electrical conductivity distribution within the volume. In the case of ground probing, an array of electrodes is placed on the ground surface to provide an image of the conductivity distribution below the surface. The EIT technology will detect mines buried in the ground by detecting ground conductivity anomalies. The presence of a metal or plastic mine will disturb the conductivity distribution in the soil. The signal characteristics are based on the size, shape, conductivity and depth of the buried mine.

Figure 1 illustrates the components of the detector system. The three major components of the EIT detector are the electrode array, the data acquisition system and the data processing application. They are described in more details in the following subsections.

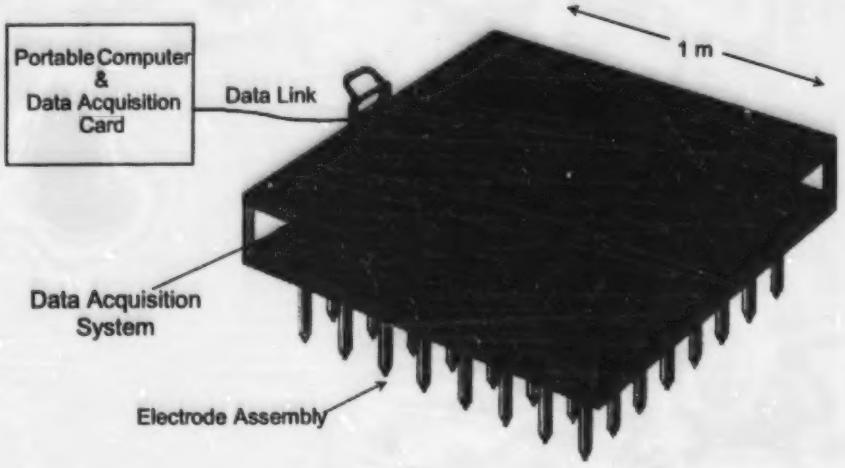

Figure 1 EIT Detector System

2.1 Electrode Array.

The Electrode Array Assembly is made of two Plexiglas plates (12.7 mm thick), held together by 8 stainless steel support rods (9.52 mm diameter). The assembly is used to hold the individual electrode assemblies in place and to support the metal enclosure containing the data acquisition electronics. The plates are square, with dimensions of 110 x 110 cm and are held 15 cm apart. The spacing between the electrodes is set at 14 cm and the array is arranged in 8 rows of 8 columns. The individual electrode assemblies are spring-loaded and can move vertically between the two plates in order to comply with the terrain variations.

John.McFee@dres.dnd.ca; phone (403) 544-4739; fax (403) 544-4704; Defence Research Establishment Suffield (DRES), Box 4000, Medicine Hat, AB, Canada, T1A 8K6.

The details of the individual electrode assembly are shown in Figure 3. Each electrode is made of a threaded stainless steel rod, 6.35 mm in diameter and 31 cm in length. Most of the electrode surface is covered with a PVC tube to keep the electrode shaft electrically insulated. An electrode tip, made of stainless steel and shown to the right of Figure 3, is installed at the end of the electrode shaft. The shape of the electrode tip was designed to reach the soil top layer for commonly found soil surface covers, such as, grass, weed and hard crust. It was determined experimentally that when a force of about 6.7 N (1.5 lb.) is applied over that type of electrode, a reliable electrical contact is usually established with the soil.

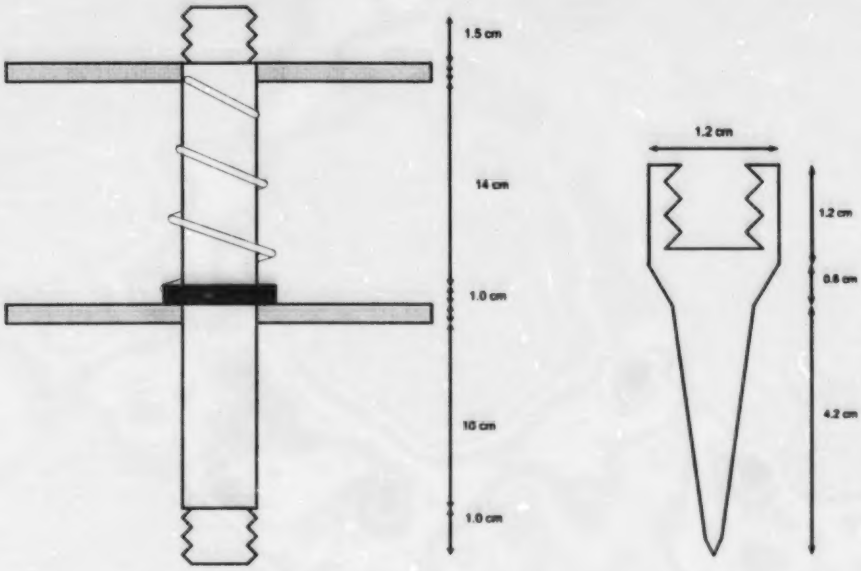

Figure 3. Individual Electrode Assembly.

2.2 Data Acquisition System.

The Data Acquisition system incorporates the electronics and firmware required for the electrical stimulation of the electrodes and the recording of the resulting potentials. The electronics is housed in a sealed anodized aluminum enclosure, mounted on the electrode array structure. The EIT instrument is a high precision impedance meter. It uses four electrodes to perform a transfer impedance measurement. Two electrodes are used to inject a current (I) in the medium and two others to measure the potential difference (V) developed on the medium surface. The transfer impedance is given by V/I.

A high level diagram of the data acquisition electronic circuit is given in Figure 4. The EIT data acquisition electronics is physically partitioned into three main subsystems: the switching logic which selects the stimulating and recording electrode configurations, the signal preprocessing circuitry, which applies a gain and filters the incoming signals, and finally the control and measurement subsystem that generates all necessary signals for the system to work. Those subsystems are designated respectively as Active Electrodes, Interface Board and Data Acquisition Board. The Data Acquisition Board is a 12-bit PCMCIA data acquisition card (DT7102) that fits in a laptop. All necessary signals are generated from that card. The Active Electrode boards and the Interface Board are located in the waterproof enclosure on top of the array. Each Active electrode board controls up to 16 electrodes and these boards can be daisy-chained. The electronic enclosure contains 4 boards for a total of 64 electrodes. The interface board powers those boards and relays the control signals coming from the computer. It also filters the analog signals before they get to the acquisition board. A battery and DC/DC converters are located inside the enclosure to provide the power. The DC/DC converter is used to provide ±12 Volts for the

analog circuitry. An external cable is used to recharge the battery. The interconnection arrangement is shown on Figure 5.

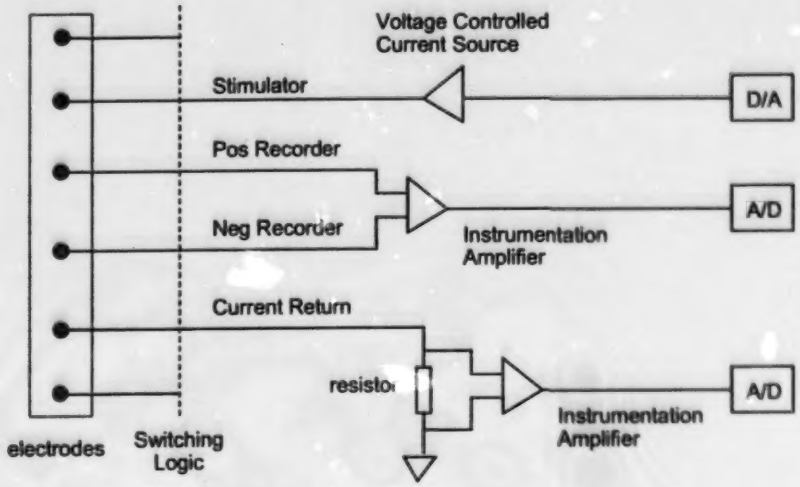

Figure 4. High level circuit diagram for the data acquisition electronics

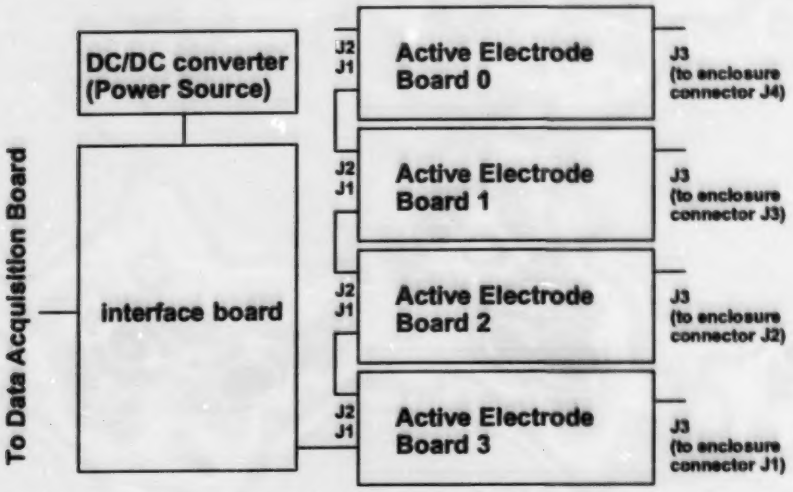

Figure 5. Block diagram illustrating the interconnection of the main data acquisition electronic boards

The medium is stimulated with a square wave of low frequency (~1kHz). The stimulation sequence is shown on Figure 6. For each configuration (a set of four electrodes, stimulating and recording) a square wave is generated to excite the medium. Then N samples are collected to measure the voltage difference between both recording electrodes and N samples are collected to measure the current injected. The default number of samples N is set to 100, (50 during the stimulation on the positive polarity and 50 during the stimulation on the negative polarity). The data acquisition card is capable of a 200 KHz sampling rate.

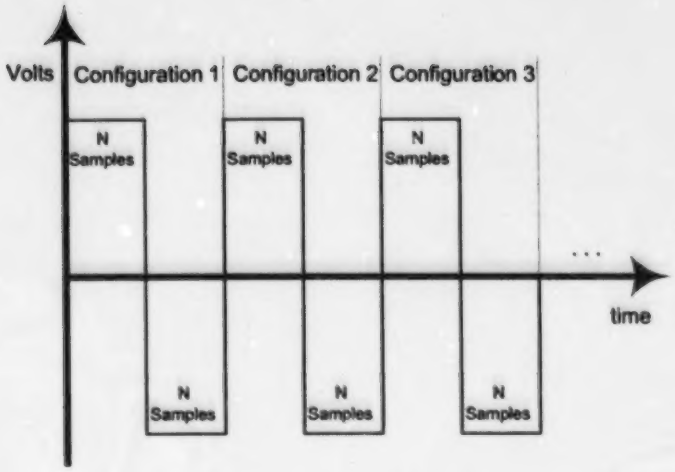

Figure 6. Stimulation sequence

For each configuration, transfer impedance estimates, Z, are formed according to expression (2-1) below, and are averaged over the total number of samples:

$$Z = \frac{V_+ - V_-}{I_+ - I_-}, \tag{2-1}$$

where, I_+ and I_- are the positive and negative stimulation currents and V_+ and V_- are the resultant potentials. This measurement method eliminates the electrode polarization voltage that usually appears as a bias voltage on the recording electrodes. This method is successful because the polarization phenomenon varies slowly in time compared to the acquisition speed. When constructing the configuration sequence, care has to be taken not to do voltage measurements on electrodes that have been recently stimulated since it breaks that assumption. This is because the polarization voltage on a stimulated electrode drops off quite rapidly just after the voltage is removed and then decreases very slowly thereafter. Avoiding making a measurement with an electrode, which has just been stimulated, prevents the measurement from being done in the phase where the polarization voltage varies rapidly. The set of configurations used for the measurements are a variation of the method initially proposed by Barber and Brown for EIT instruments [4]. For this particular instrument a total of 1698 independent configurations are used.

2.3 Data Processing Application

The data processing application comprises the software required for the data acquisition and the target detection algorithm. A laptop computer (IBM ThinkPad) is the host computer. The basic algorithm developed for the reconstruction of the electrical conductivity distribution is described in detail in [3]. It is a linearized reconstruction based on the following relation:

$$\delta z \sim S\delta\sigma \tag{2-2}$$

The terms are defined as follows:

δZ: The elements of this vector represent the difference between the transfer impedance measurement for a given configuration of pairs of stimulators and recorders and the transfer impedance predicted by an homogeneous, semi-infinite model for the same configuration. The size of the vector is determined by the number of independent measurements used by the system.

S: This is defined as the sensitivity matrix. Its form arises from a linear approximation and its elements are evaluated by averaging, over a grid cell, the scalar product of the electric field caused by the stimulating electrodes with the electric field that would result if the recording pair were stimulated.

$\delta\sigma$: The elements of this vector represent the conductivity perturbation (with respect to the uniform conductivity, semi-infinite model) over a regular grid covering the region of interest. This is the solution that is referred to as the "conductivity distribution reconstruction".

The solution to equation (2-2) requires the inverse of S. The matrix is ill-conditioned and requires a regularization procedure in order to calculate its inverse. The inverse will be defined as:

$$S^{-1} \sim S^{\#} \tag{2-3}$$

Because of the regularization procedure, $S^{\#}$ can only be an approximation of S^{-1}. The conductivity reconstruction is therefore given by:

$$\delta\sigma \sim S^{\#}\delta z \tag{2-4}$$

Expression (2-4) is used as the basis of a detection algorithm that can be tuned to a specific type of mine, based on its shape and size. This is important for an EIT mine detector because the detection algorithm can reduce the number of false alarms.

The mine detection algorithm is based on a matched filter approach. It consists of calculating the detector response for a replica of the size and shape of the object of interest, for a number of grid locations underneath the detector. The detector response, for a given replica, is calculated by assigning a zero conductivity to the nodes of the calculation grid that represent the size and shape of the replica. A correlation is then performed between the detector response for the replica and the actual detector response obtained from the measurements, for all the replica positions considered. The position that yields the largest correlation value is identified as the most likely position for the mine.

A grid with a resolution of 15x15x3 nodes is used for the calculations. This resolution is equivalent to 0.5 electrode spacing (7 cm), in x, y and z. For every node i of that grid, the correlation operation is defined by the following scalar product:

$$\delta\sigma_r^i \,.\, \delta\sigma, \tag{2-5}$$

where $\delta\sigma_r^i$ is the detector response for a replica, at position i, and $\delta\sigma$ is the detector response for the present set of measurements. Using equation (2-4), the expression (2-5) can be expressed as an operator on the measurement vector.

$$\delta\sigma_r^i \sim S^{\#}\delta z_r^i, \tag{2-6}$$

where δz_r^i is the vector whose elements are the difference between the transfer impedance values calculated with the replica at position i and the transfer impedance values calculated with the homogenous model. The terms δz_r^i are calculated using expression (2-2), and using one unit of conductivity for the conductivity perturbation at the positions occupied by the replica on the calculation grid. Using expressions (2-6) and (2-4) in equation (2-5) we obtained:

$$\delta\sigma_r^i \,.\, \delta\sigma = (S^{\#}\delta z_r^i)^T S^{\#}\delta z \tag{2-7}$$

A detection operator, D^i, can now be defined using (2-7) for a replica at position i:

$$D^i = (S^{\#}\delta z_r^i)^T S^{\#} \tag{2-8}$$

A matrix D is then generated for every node i of the calculation grid. The matched filter is defined by applying D to the measurement vector δz and normalizing the expression by the detector response obtained from a uniform

conductivity perturbation, i.e., the response obtained after assigning a conductivity perturbation of one unit at each node of the calculation grid. The normalized matched filter, C, is defined as follows:

$$C = D\,\delta z / D\,\delta z', \tag{2-9}$$

where $\delta z'$ is the detector response obtained for a uniform conductivity perturbation $\delta\sigma'$, and is calculated using expression (2-2).

The detection calculations were done using a grid comprising 675 node points and 1698 independent measurements. For that application, δz is column vector with a size of 1698 elements, D is matrix with a size of 675x1698 and C is column vector with 675 elements. D is pre-calculated and if there are more than a single target of interest, several operators D can be made available for each type of target. In the context of this work, the replicas were representative of the size and shape of the mine-like objects used for the tests.

3. FIELD EVALUATIONS

The EIT detector was subjected to a preliminary evaluation in the vicinity of Computing Devices Canada (CDC, Ottawa) and was then evaluated at Defence Research Establishment Suffield (DRES). The CDC evaluation was done over a sandy terrain with an electrical conductivity of the order of 2 mS/m. The DRES evaluation was done in a terrain made of loam with an electrical conductivity of the order of 15 mS/m.

3.1 Detection versus depth

Figure 7, Figure 8 and Figure 9 illustrate the detector performance obtained for an AT mine-like object buried at 7, 14 and 21 cm. The AT mine-like object, in this case, is a circular plastic container with a diameter of 28 cm and a thickness of 12 cm. Each figure represents the results of the matched filter algorithm as per (2-9). The 3D plot represents the intensity of the matched filter detection as a function of the positions in the x-y plane, in units of meters. The plot on the left is a color-coded projection of the detector response onto the x-y plane. This 2D representation helps understand the contour and the extent of the detector response. For all cases, the detector response is calculated at a grid layer located 14 cm down from the electrode array.

3.2 Detector Spatial Resolution

Experiments have been done to evaluate the resolution capability of the detector using two mine-like objects buried in close proximity. Figure 10 illustrates the detector response for two AT mine-like objects buried at a depth of 14 cm and separated by 7 cm. The separation distance corresponds to the shortest distance between the edges of the two objects. Figure 12 illustrates the detector response for two AT mine-like objects buried at a depth of 21 cm and separated by 14 cm. The mine-like objects were identical to the ones described above.

3.3 Detector response to various AT mine types

Trials were conducted at the DRES Mine Pen facility. The first set of experiments were performed on a hard packed gravel road containing various buried landmines. The EIT detector was used to image several inert AT mines buried at different depths. Table 1 lists the dimensions of the AT mines used for the tests. Figure 13 shows the detector response for a TMA3 nonmetallic AT mine, buried at a depth of 6.4 cm. Figure 14 shows the detector response for a M15 metal AT mine, buried at a depth of 16.5 cm. Figure 15 shows the detector response for a PtMiBalII nonmetallic AT mine buried at a depth of 6.4 cm. Figure 16 shows the detector response for a TMA4 non-metallic AT mine buried at a depth of 19.1 cm.

AT Mine	Diameter (cm)	Thickness (cm)
TMA3	26.5	10.0
M15	33.7	15.0
PtMiBalII	33.0	10.7
TMA4	28.0	6.5

Table 1. AT Mines tested at the DRES facility

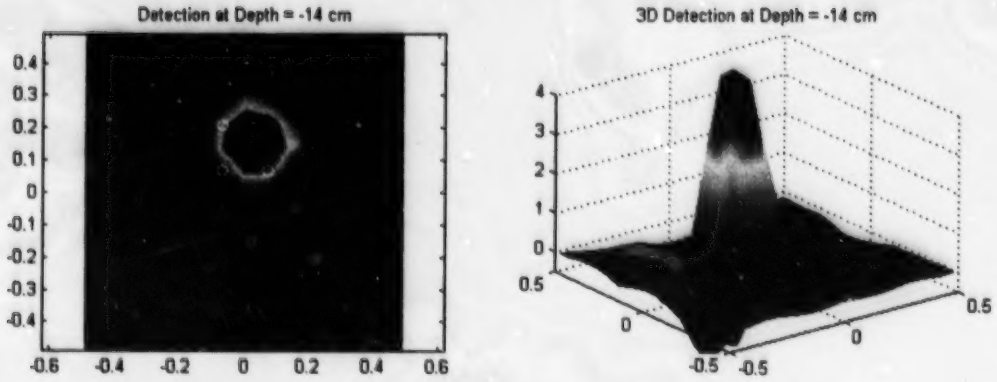

Figure 7. Detector response for a mine-like object buried at a depth of 7 cm

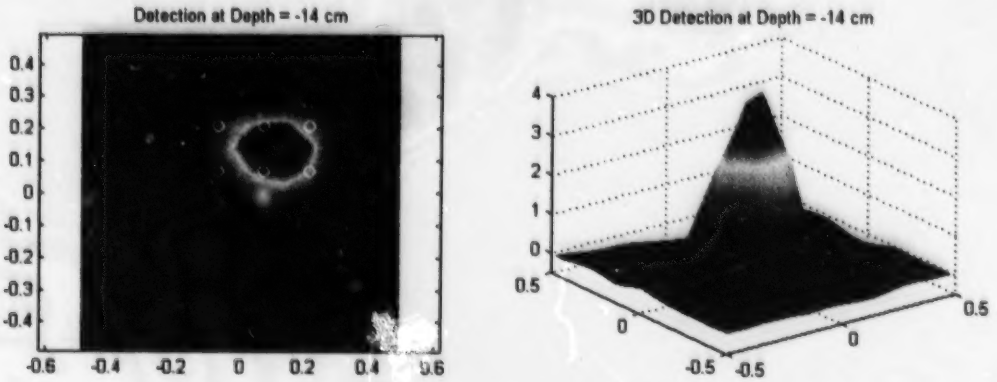

Figure 8. Detector response for a mine-like object buried at a depth of 14 cm

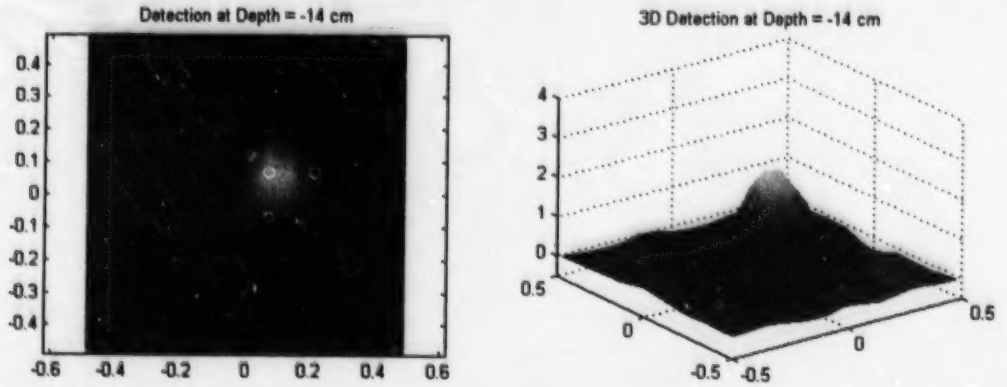

Figure 9. Detector response for a mine-like object buried at a depth of 21 cm

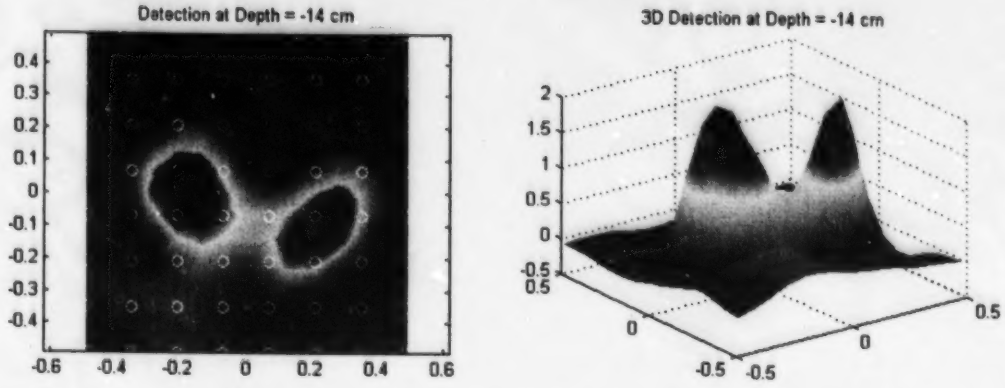

Figure 10. Detector response for two mine-like objects buried at 14 cm (7 cm separation)

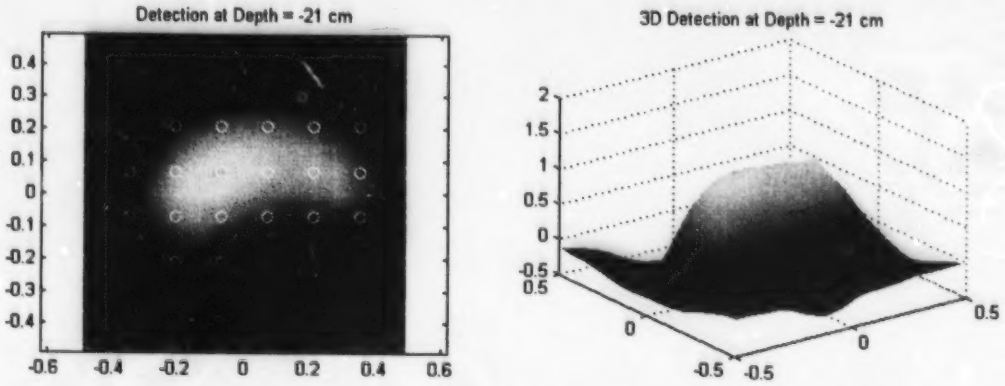

Figure 12. Detector response for two mine-like objects buried at 21 cm (14 cm separation)

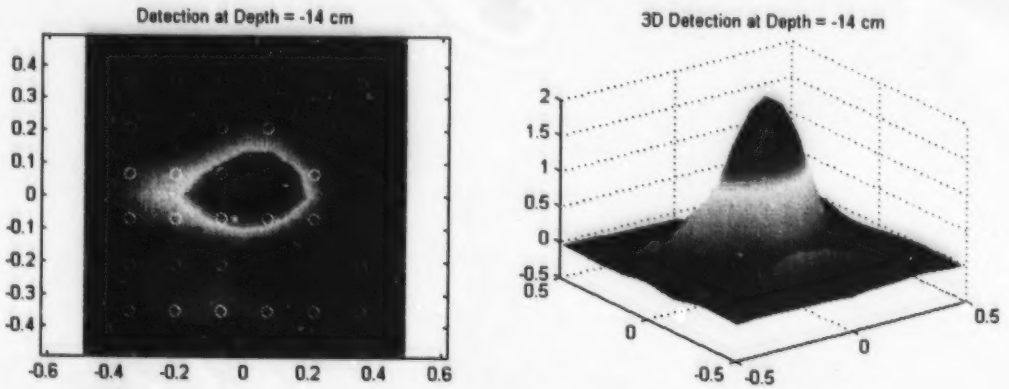

Figure 13. Detector response for a TMA3, buried at a depth of 6.4 cm

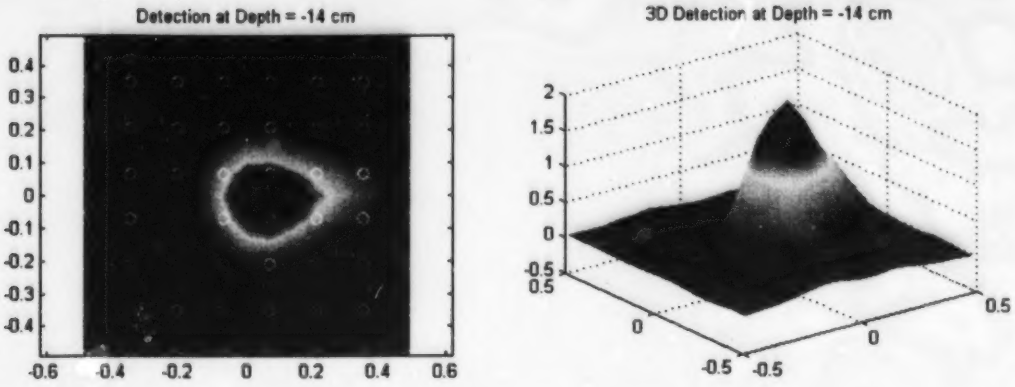

Figure 14. Detector response for a M15, buried at a depth of 16.5 cm

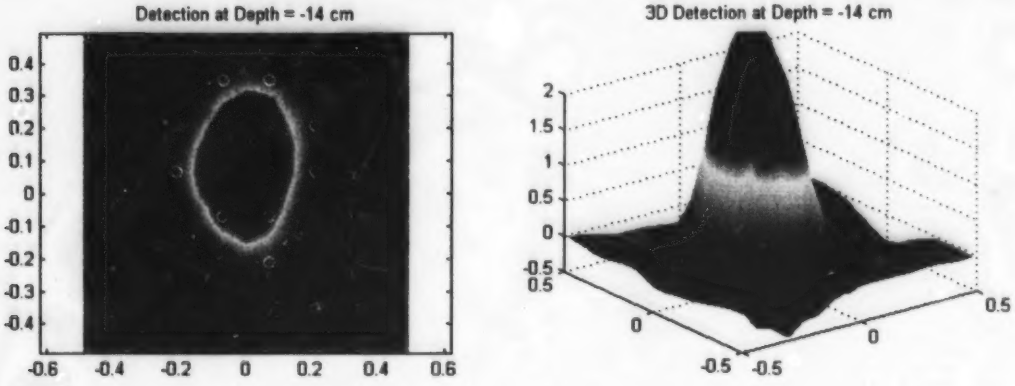

Figure 15. Detector response for a PTMiBAIII, buried at a depth of 6.4 cm

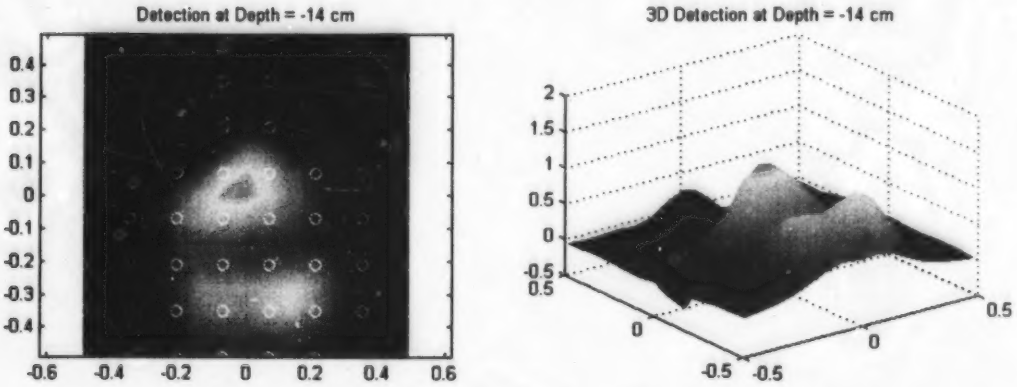

Figure 16. Detector response for a TMA4, buried at a depth of 19.1 cm

4. RESULTS DISCUSSION

Using mine-like objects with a size of the order of two electrode-spacings (ES), reliable detections were obtained down to a range of 1.0-1.5 ES. For an AT mine with a 28 cm diameter, this results in a detection range of about 15-20 cm in depth. The detection of targets down to a depth of 17 cm has been successful in all cases. The strength of the detection varies for targets buried at depths of 21 cm (1.5 ES). This performance has been consistent with the whole set of experiments that have been performed in various soils, either with the small scale lab model used in the initial phase of investigation [3] or with the current 64 electrode instrument.

The detector was found capable of resolving very well two mine-like objects buried at 1 ES and separated by 0.5 ES. For two AT mines with a 23 cm diameter and buried at a depth of 14 cm, this corresponds to a distance of 7 cm separating the edges of the two objects (35 cm center-to-center). The resolution of two mine-like objects buried at 1.5 ES and separated by 1 ES was not successful, indicating that the resolution power of the detector decreases rapidly with the depth of burial.

The EIT detector performed unexpectedly well in the DRES Mine Pen facility. The hard soil crust, covered with small pebbles was thought to be too difficult to achieve a good electrode-soil contact. AT mines (TMA3, M15, PTMiBAIII) were clearly detected, down to depth of 16 cm. The detector's response for the TMA4 buried at 19 cm was not as clear as for the other mines, the detector being at the limit of its detection capability for that depth level. The metal AT mine M16 was detected as a non-conductive object, presumably because of its coat of paint. The same behaviour had been observed for the metal mine TM46 during the trials at CDC.

Another set of experiments was carried along an alley of surrogate AT mines set up at DRES. The results presented unexpected anomalies. The signal from the surrogate AT mine was weaker than expected and the detector was often showing a strong and broad signal at the lower layers. These anomalies may actually be related in the sense that the broad signal is masking the features we were trying to detect. It appears that the ground environment is likely responsible for the problems encountered. The results from experiments point to the presence of a double layer of soil, having different electrical conductivities. The current conductivity reconstruction algorithm assumes a conductivity perturbation in a semi-infinite homogeneous medium. The algorithm requires a revision in order to work properly in environments that present multi-layers of soils having very different conductivities.

5. CONCLUSION

This work concludes a two-phase study on the suitability of using EIT technology as the basis of a confirmatory detector for AT mines. As a very general conclusion, the EIT technology has proven to be useful in the role of a confirmatory detector for AT mines. This has been proven through the experiments in the DRES Mine Pen facility. Results from the trials at CDC and DRES have also indicated the detector is capable of reliably detecting AT type mines at depths of the order of 15-20 cm. The detector is also capable of resolving typical AT size mine buried at depths of up to 16 cm and separated by distances as small as 7 cm. A detection algorithm based on replica of the object of interest has also proven to be efficient in reducing the false alarm rate of the detector. The trials performed at DRES have also shown that the soil environment may impact significantly on the detector performance if this is not accounted for in the reconstruction model.

However, in order to provide a balanced evaluation of the EIT detection technology, it should be pointed out that the detector also faces limitations because an electrode-soil contact is required. Electrical contact cannot be assured in all type of environments and the deployment of electrodes in close proximity of explosives is a potential operational issue, although no large force is required to achieve contact.

The EIT technology, as a mine detection application, appears to have a special niche in environments such as beaches, ocean littorals and other wet areas. This is because this is where EIT works at its best. The detector has proven to be unexpectedly efficient in the sand, even if it is poorly conductive, as long as the sand holds a bit of moisture. The fluidity of the sand also provides an easy, reliable contact with the electrodes. EIT may also

have an application in locating intact mines in the berms formed when mine clearing equipment neutralizes and removes mines. Most mines in such berms are already inert, reducing the likelihood of an initiation when inserting the sensor head. Further, the EIT sensor head could be made cheaply enough to be disposable and remotely inserted to improve safety.

6. REFERENCES

[1] Wexler A., "Electrical Impedance Imaging in Two and Three Dimensions", Clinical Physics and Physiological Measurement , Suppl. A., pp 29-33,1988.

[2] Wexler A., Fry B., Neuman M.R., "Impedance-Computed Tomography Algorithm and System", Applied Optics 24, pp. 3985-3992, Dec. 1985.

[3] Wort P., Church P., Gagnon S., "Preliminary Assessment of Electrical Impedance Tomography Technology to Detect Mine-like Objects", Proceedings of SPIE Conference on Detection and Remediation of Mines and Mine-like Targets IV, Vol. 3710, Orlando FL USA, 5-9 April 1999, pp.895-905.

[4] Brown B., Barber D., Freeston I., US Patent Number 4,617,939, Oct., 1986.

7. ACKNOWLEDGMENTS

This work was performed at Computing Devices Canada, with the partial financial support of Defence Research and Development Canada, Project 2mf.